

Photo-Gated Charge Transfer of Organized Assemblies of CdSe Quantum Dots

Sulolit Pradhan,[†] Shaowei Chen,^{*,†} Shizhong Wang,[‡] Jing Zou,[‡]
Susan M. Kauzlarich,^{*,‡} and Angelique Y. Louie[§]

Department of Chemistry and Biochemistry, University of California—Santa Cruz,
Santa Cruz, California 95064, Department of Chemistry, and Department of Biomedical Engineering,
University of California—Davis, Davis, California 95616

Received July 11, 2005. In Final Form: November 7, 2005

The electronic conductivity of tri-*n*-octylphosphineoxide (TOPO)-protected CdSe quantum dots (QDs) was studied at the air–water interface using the Langmuir technique within the context of photochemical and photophysical excitation. It was found that, upon photoirradiation with photon energies higher than that of the absorption threshold, the voltammetric currents increased rather substantially with a pair of voltammetric peaks at positive potentials. However, the photoconductivity profiles exhibited a dynamic transition, which was ascribed to the strong affinity of oxygen onto the CdSe surface and the consequent trapping of the photogenerated electrons. The resulting excess of holes led to photocorrosion of the particle cores. The oxygen adsorption and photoetching processes were found to be reversible upon cessation of the photoexcitation. In contrast, only featureless voltammetric responses were observed when the particle monolayers were deposited onto the electrode surface and the film conductance was measured in a vacuum (the overall profiles were analogous to that of a Coulomb blockade). A comparative study was also carried out with a CdSe dropcast thick film immersed in acetonitrile, where the photoconductivity profiles were reversible and almost linear. The latter was attributed to the separation of photogenerated electrons and holes which were subsequently collected at the electrodes under voltammetric control. In the dropcast system, the oxygen effects were minimal which was ascribed to the acetonitrile medium that limited the access to oxygen and thus the particles were chemically intact. These studies suggest that chemical environment plays an important role in the determination of the chemical stability and electronic conductivity of CdSe QD thin films.

Introduction

The intense research interest in nanoparticle materials has been driven mainly by their size-dependent electronic, optical, magnetic, and catalytic properties that differ vastly from their bulk counterparts.^{1–4} Of these nanoparticle materials, semiconductor quantum dots (QDs) exhibit unique optoelectronic properties that may be exploited in the fabrication of novel sensors, photovoltaics, functional devices, and electronic circuits, etc.^{5–10} For instance, Bard et al.^{11–15} has showed that a variety of

semiconductor particles exhibited interesting electrogenerated chemiluminescence (ECL) properties. Work by Greenham et al.¹⁶ demonstrated that the charge separation and transport of conjugated polymer/nanocrystal composites could be controlled by the chemical structure of the nanocrystals in photoluminescence (PL) and photoconductivity measurements. Photoconductivity of PbS nanocrystals/polymer composites^{17,18} has also been studied for infrared photodetection and photovoltaic applications, and electrochromic changes have been observed for CdSe nanocrystal thin films.¹⁹ The interconversion and intrinsic relation between electronic and optical responses in these materials are the fundamental basis on which optoelectronic device applications are possible.

The chemical stability of the QD molecules can also have significant effects on their photo- and electrochromic properties, especially for II–VI semiconductor QDs. It has been found that under photoirradiation, adsorption of ambient oxygen onto the particle surface leads to the efficient trapping of photogenerated electrons and hence an excess of holes in the particles.^{20–23} This then causes oxidation and photocorrosion of the particle cores,

* To whom all correspondence should be addressed. E-mail: schen@chemistry.ucsc.edu (S.C.); smkauzlarich@ucdavis.edu (S.M.K.).

[†] University of California, Santa Cruz.

[‡] Department of Chemistry, University of California—Davis.

[§] Department of Biomedical Engineering, University of California—Davis.

(1) Schmid, G. *Nanoparticles: from theory to application*; Wiley-VCH: Weinheim, Germany, 2004.

(2) Turton, R. *The quantum dot: a journey into the future of microelectronics*; Oxford University Press: New York, 1995.

(3) Yoffe, A. D. *Adv. Phys.* **2001**, *50*, 1–208.

(4) Schmid, G. *Clusters and colloids: from theory to applications*; VCH: Weinheim, Germany, 1994.

(5) Colvin, V. L.; Schlamp, M. C.; Alivisatos, A. P. *Nature* **1994**, *370*, 354–357.

(6) Coe, S.; Woo, W. K.; Bawendi, M.; Bulovic, V. *Nature* **2002**, *420*, 800–803.

(7) Hikmet, R. A. M.; Talapin, D. V.; Weller, H. *J. Appl. Phys.* **2003**, *93*, 3509–3514.

(8) Bruchez, M.; Moronne, M.; Gin, P.; Weiss, S.; Alivisatos, A. P. *Science* **1998**, *281*, 2013–2016.

(9) Chan, W. C. W.; Nie, S. M. *Science* **1998**, *281*, 2016–2018.

(10) Mattoussi, H.; Mauro, J. M.; Goldman, E. R.; Anderson, G. P.; Sundar, V. C.; Mikulec, F. V.; Bawendi, M. G. *J. Am. Chem. Soc.* **2000**, *122*, 12142–12150.

(11) Ogawa, S.; Hu, K.; Fan, F. R. F.; Bard, A. J. *J. Phys. Chem. B* **1997**, *101*, 5707–5711.

(12) Myung, N.; Ding, Z. F.; Bard, A. J. *Nano Lett.* **2002**, *2*, 1315–1319.

(13) Myung, N.; Bae, Y.; Bard, A. J. *Nano Lett.* **2003**, *3*, 747–749.

(14) Myung, N.; Lu, X. M.; Johnston, K. P.; Bard, A. J. *Nano Lett.* **2004**, *4*, 183–185.

(15) Bae, Y.; Myung, N.; Bard, A. J. *Nano Lett.* **2004**, *4*, 1153–1161.

(16) Greenham, N. C.; Peng, X. G.; Alivisatos, A. P. *Phys. Rev. B—Condensed Matter* **1996**, *54*, 17628–17637.

(17) McDonald, S. A.; Cyr, P. W.; Levina, L.; Sargent, E. H. *Appl. Phys. Lett.* **2004**, *85*, 2089–2091.

(18) McDonald, S. A.; Konstantatos, G.; Zhang, S. G.; Cyr, P. W.; Klem, E. J. D.; Levina, L.; Sargent, E. H. *Nat. Mater.* **2005**, *4*, 138–U14.

(19) Guyot-Sionnest, P.; Wang, C. J. *Phys. Chem. B* **2003**, *107*, 7355–7359.

(20) Spanhel, L.; Haase, M.; Weller, H.; Henglein, A. *J. Am. Chem. Soc.* **1987**, *109*, 5649–5655.

(21) Koberling, F.; Mews, A.; Basche, T. *Adv. Mater.* **2001**, *13*, 672–676.

(22) Aldana, J.; Wang, Y. A.; Peng, X. G. *J. Am. Chem. Soc.* **2001**, *123*, 8844–8850.

(23) van Sark, W. G. J. H. M.; Frederix, P. L. T. M.; van den Heuvel, D. J.; Bol, A. A.; van Lingen, J. N. J.; Donega, C. D.; Gerritsen, H. C.; Meijerink, A. *J. Fluoresc.* **2002**, *12*, 69–76.

which effectively results in the shrinkage of the particle core dimension and a blue shift of the emission profiles.^{20–23} Also interesting is the so-called photoactivation process that accompanies the photoetching phenomena where prolonged illumination in the presence of oxygen leads to drastic enhancement of the QD quantum efficiency reflected in ECL and PL measurements. In addition, with the resulting positively charged particles, the photogenerated electron–hole pairs predominantly recombine nonradiatively which may be the controlling mechanism for the blinking of the QD molecules in single molecule spectroscopic measurements.^{20–23} Numerous related studies have been carried out on CdSe QDs mainly because of the well-established synthetic protocols^{24–27} and the well-known photochemistry of the bulk materials.^{28–30}

Electrochemical manipulation has been found to be another effective tool in controlling the QD chemical stability and hence their optoelectronic properties, especially in combination with photoexcitation.^{31–35} Typically, for II–VI semiconductors, the compound molecules will undergo electrodegradation at positive and/or negative potentials under ambient conditions.^{31–33,35} The exact potentials are determined by the electronic energy structures of the semiconductor materials. Such decomposition reactions may be accelerated by photoirradiation and generally not electrochemically reversible. The corresponding voltammetric responses can be exploited to evaluate the effective band gap energies of nanoparticle molecules and ensembles.

In this article, we report an electrochemical study of CdSe QD arrays where the voltammetric currents can be gated by photoexcitation. Our focus is to investigate the effects of QD chemical stability, photoexcitation, and chemical environments on the conductivity properties of the QD ensembles. Two approaches are employed to prepare the particle assemblies. The first entails the Langmuir technique where a monolayer of CdSe QDs is formed on the water surface and an interdigitated arrays (IDAs) electrode is aligned vertically at the air–water interface for in situ voltammetric measurements at varied interparticle separations. Such an approach has been used previously to investigate the ensemble electronic conductivity properties of metal and semiconductor nanoparticles^{31–33} as well as single-walled carbon nanotubes.³⁴ The second method involves drop-casting a QD solution onto the surface of an interdigitated arrays (IDAs) electrode forming a (sub) μm thick film. Previous work on metal nanoparticles has shown that the dropcast thick films demonstrate rather significantly different voltammetric behaviors as compared to those of the Langmuir monolayers, which was ascribed mainly to the structural defects in the particle dropcast films that facilitate facile charge transfer.^{36–41}

In the present study, we also observe very different photoconductivity properties of the CdSe QD assemblies prepared by the Langmuir and dropcast methods. The discrepancy is explained within the context of structural defects in the particle solid thin films, and their photochemical/physical activities, in particular, oxygen effects on photocharge transfer (i.e., charge trapping and separation). The latter is further examined by comparing results with those measured in vacuo where a particle monolayer is deposited onto the electrode surface by the Langmuir–Blodgett technique.

Experimental Section

Materials. Trioctylphosphine oxide (TOPO, 99%, ACROS), trioctylphosphine (TOP, 90%, Aldrich), hexadecylamine (HDA, 98%, Aldrich), selenium (Se, 99.5+%, ACROS), and cadmium acetate (CdAc_2 , 98%, ACROS) were used as received. All solvents were purchased from typical commercial vendors and used as received as well. Water was provided by a Barnstead Nanopure Water Purification System ($\geq 18 \text{ M}\Omega$).

Synthesis of TOPO-Capped CdSe Nanoparticles. CdSe nanoparticles were synthesized by using a previously described method.⁴² Briefly, 8 g of trioctylphosphine oxide (TOPO) was dried and degassed under vacuum in a 250 mL flask at 200 °C for 30 min. The TOPO was then cooled to 120 °C, and 5 g of hexadecylamine (HDA) powder was added under flowing argon. The mixture was degassed again at 140 °C for another 30 min. Then the mixture was put under an Ar atmosphere. To this mixture, a stock solution of selenium (0.158 g, 2.0 mmol) dissolved in 3 mL of trioctylphosphine (TOP) was injected. The mixture was then heated to 300 °C under vigorous stirring, and was then injected with another stock solution of cadmium acetate (0.12 g, 0.5 mmol) dissolved in 2 mL of TOP. The temperature was then decreased to 260 °C and maintained for 15 min before cooling down to room temperature for the crystal growth of CdSe (the growth time was about 1 h).

CdSe nanoparticles were then isolated and washed with a solvent pair of chloroform and methanol for three times to remove the free ligands of TOPO, HDA, and TOP.⁴³ Finally, the isolated CdSe nanoparticles were dissolved and stocked in chloroform.

Transmission Electron Microscopy. The size of CdSe nanoparticles was investigated using a transmission electron microscope (TEM, Phillips CM-12) at an accelerating voltage of 100 kV. The TEM samples were prepared by the evaporation of the colloids on holey and continuous carbon-coated 400-mesh electron microscope grids followed by heating at 120 °C overnight. The size analysis of nanoparticles was performed with the commercial software, Analysis.

Spectroscopies. UV–visible spectroscopic measurements were carried out with a UNICAM ATI UV4 spectrometer, whereas fluorescence properties were characterized with a PTI Fluorescence Spectrometer. The typical concentration of the QD solution was 0.27 μM and the same solution was used both in the UV–vis and fluorescence measurements. The quantum yield (QY) of these CdSe QDs is $\sim 16\%$ by using Rhodamine B in ethanol as a calibration reference.

Electrochemistry. Electrochemical measurements were carried out in two QD structures. The first involved the preparation of a Langmuir monolayer of QD molecules at the air–water interface. This experimental setup has been described in detail previously^{31–34} (Scheme 1). In a typical experiment, 220 μL of a CdSe–TOPO particle solution (2.75 μM in CHCl_3) was spread dropwise onto the water

(24) Steigerwald, M. L.; Alivisatos, A. P.; Gibson, J. M.; Harris, T. D.; Kortan, R.; Muller, A. J.; Thayer, A. M.; Duncan, T. M.; Douglass, D. C.; Brus, L. E. *J. Am. Chem. Soc.* **1988**, *110*, 3046–3050.

(25) Carr, D. W.; Evoy, S.; Sekaric, L.; Craighead, H. G.; Parpia, J. M. *Appl. Phys. Lett.* **2000**, *77*, 1545–1547.

(26) Alivisatos, A. P. *J. Phys. Chem.* **1996**, *100*, 13226–13239.

(27) Qu, L. H.; Peng, Z. A.; Peng, X. G. *Nano Lett.* **2001**, *1*, 333–337.

(28) Park, S. M.; Barber, M. E. *J. Electroanal. Chem.* **1979**, *99*, 67–75.

(29) Szabo, J. P.; Cocivera, M. *J. Electroanal. Chem.* **1988**, *239*, 307–319.

(30) Singh, K.; Mishra, S. S. D. *Solar Energy Mater. Solar Cells* **2000**, *63*, 275–284.

(31) Chen, S. W. *Anal. Chim. Acta* **2003**, *496*, 29–37.

(32) Greene, I. A.; Wu, F. X.; Zhang, J. Z.; Chen, S. W. *J. Phys. Chem. B* **2003**, *107*, 5733–5739.

(33) Yang, Y. Y.; Pradhan, S.; Chen, S. W. *J. Am. Chem. Soc.* **2004**, *126*, 76–77.

(34) Yang, Y. Y.; Chen, S. W.; Xue, Q. B.; Biris, A.; Zhao, W. *Electrochim. Acta* **2005**, *50*, 3061–3067.

(35) Haram, S. K.; Quinn, B. M.; Bard, A. J. *J. Am. Chem. Soc.* **2001**, *123*, 8860–8861.

(36) Wuelfing, W. P.; Murray, R. W. *J. Phys. Chem. B* **2002**, *106*, 3139–3145.

(37) Wuelfing, W. P.; Green, S. J.; Pietron, J. J.; Cliffel, D. E.; Murray, R. W. *J. Am. Chem. Soc.* **2000**, *122*, 11465–11472.

(38) Evans, S. D.; Johnson, S. R.; Cheng, Y. L. L.; Shen, T. H. *J. Mater. Chem.* **2000**, *10*, 183–188.

(39) Doty, R. C.; Yu, H. B.; Shih, C. K.; Korgel, B. A. *J. Phys. Chem. B* **2001**, *105*, 8291–8296.

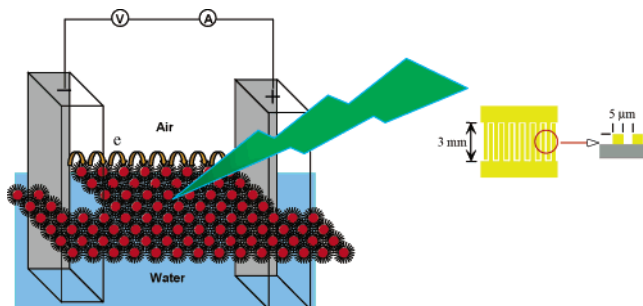
(40) Snow, A. W.; Wohltjen, H. *Chem. Mater.* **1998**, *10*, 947–950.

(41) Clarke, L.; Wybourne, M. N.; Brown, L. O.; Hutchison, J. E.; Yan, M.; Cai, S. X.; Keana, J. F. W. *Semiconductor Sci. Technol.* **1998**, *13*, A111–A114.

(42) Mekis, I.; Talapin, D. V.; Kornowski, A.; Haase, M.; Weller, H. *J. Phys. Chem. B* **2003**, *107*, 7454–7462.

(43) Murray, C. B.; Kagan, C. R.; Bawendi, M. G. *Annual Review of Mater. Sci.* **2000**, *30*, 545–610.

Scheme 1. Experimental Setup for the Solid-state Electrochemical Measurements by the Langmuir Technique^a



^a Details have been described in refs 31–34.

surface of a Langmuir–Blodgett trough (NIMA 611D; subphase resistance $\geq 18 \text{ M}\Omega$, provided by a Nanopure water system). At least 20 min was allowed for solvent evaporation prior to the first compression and between compression cycles. Compression speed was set at $10 \text{ cm}^2/\text{min}$. Prior to this, a gold interdigitated arrays (IDA) electrode (25 pairs of gold fingers of $3 \text{ mm} \times 5 \mu\text{m} \times 5 \mu\text{m}$, from ABTECH) was coated with a self-assembled monolayer of *n*-butanethiol (to render the electrode surface hydrophobic) and aligned perpendicularly at the air–water interface. The two lead contacts were connected to an EG&G PARC 283 Potentiostat, and the current–potential responses at varied surface pressures were collected using commercial softwares from EG&G. It should be noted that, in this procedure, the electronic conductivity of the nanoparticle monolayers was probed in situ at the air–water interface, and photoexcitation was introduced by shining a laser onto the particle monolayer within the IDA finger electrodes.

A comparative study was carried out by depositing the particle monolayer onto an IDA electrode surface by the Langmuir–Blodgett technique and the corresponding conductivity properties were then examined in a vacuum.

In other electrochemical measurements, a thick film of QD layers were deposited onto the IDA electrode surface by dropcasting a QD solution in CH_2Cl_2 . Typically about $5 \mu\text{L}$ of CdSe solution ($2.75 \mu\text{M}$) was deposited to cover the entire IDA finger area, on average corresponding to approximately 30 QD layers (a full monolayer is ca. $4.67 \times 10^{-12} \text{ mol}/\text{cm}^2$ by assuming a close packed structure of the QD film). This IDA electrode was then introduced into acetonitrile where the electronic conductivity of the QD films was evaluated again within the context of photoexcitation.

In these photoelectrochemical measurements, four low-power lasers (CW mode, 20–25 mW) were used, UV (355 nm, 3.50 eV), blue (473 nm, 2.63 eV), green (532 nm, 2.34 eV), and red (638 nm, 1.95 eV), all from CrystalLasers (Reno, Nevada).

Results and Discussion

Nanoparticle Structures. CdSe QD core size was evaluated by using transmission electron microscopic (TEM) measurements. Figure 1 shows a representative TEM micrograph with the size histogram in the figure inset. The particles are found to be quite uniform in shape with the average diameter at $4.80 \pm 0.60 \text{ nm}$ (from the measurements of over 700 particles). Thus, the radius of these QDs is far smaller than the exciton Bohr radius in bulk CdSe (5.4 nm),³ which indicates that the particle dimensions are in the strong quantum confinement region. Such effects can be manifested by a blue-shift of the absorption edge as compared to that of the bulk materials. Figure 2 shows the UV–visible absorption spectrum of the CdSe–TOPO particles in chloroform. A very well-defined excitonic absorption peak at 568 nm can be seen, corresponding to a HOMO–LUMO band gap of 2.2 eV. This energy is substantially greater than that of bulk CdSe (1.74 eV).¹⁷ It has been found that the blue shift of the optical absorption threshold of QD molecules can be correlated directly to the

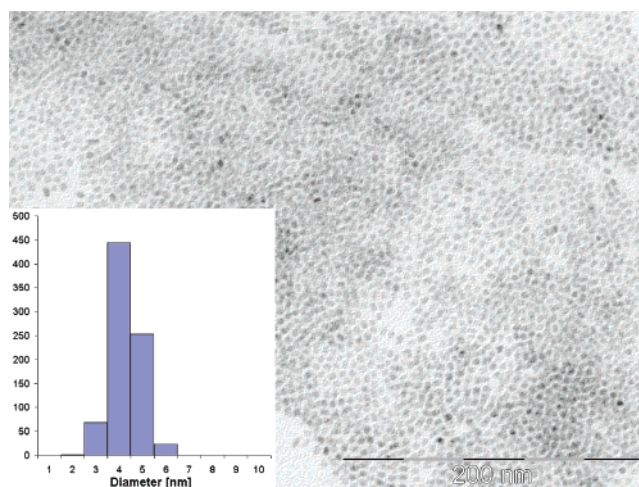


Figure 1. TEM Micrograph of CdSe–TOPO nanoparticles. Inset shows the histogram of particle core diameters.

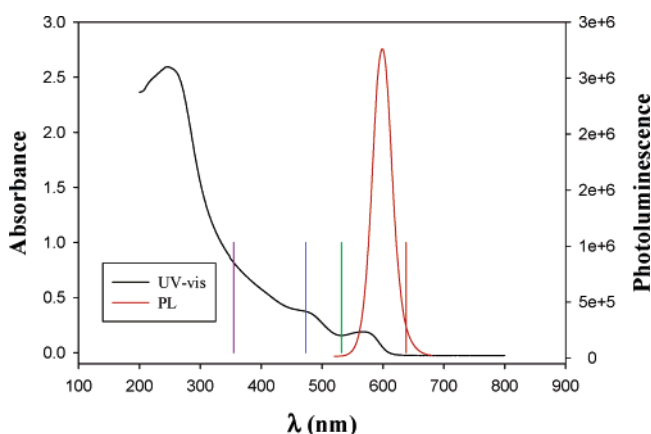


Figure 2. UV–vis absorption and photoluminescence spectra of CdSe–TOPO QDs in CHCl_3 . The fluorescence spectrum was collected with excitation wavelength at 568 nm. Particle concentration $0.27 \mu\text{M}$. The four vertical bars represent the wavelength positions of the four lasers used.

nanocrystal size⁴⁴

$$d \cong \sqrt{\frac{h^2}{2\Delta E_g} \left(\frac{1}{m_e} + \frac{1}{m_h} \right)} \quad (1)$$

where ΔE_g is the shift of QD band gap energies relative to that of bulk materials, m_e and m_h are the effective electron and hole masses respectively ($m_e = 0.13m_0$ and $m_h = 0.60m_0$ for bulk CdSe with m_0 being the electron rest mass⁴⁵), and h is the Planck's constant. Thus, from eq 1, one can estimate that the QD size is about 5.54 nm, which is somewhat larger than that from TEM measurements. It has to be noted that the result from TEM measurements is a statistical average of all particles that are imaged whereas in spectroscopic studies, the absorption profile is a combined contribution of particles of varied sizes and absorption coefficients where larger-size particles appear to be more dominating than smaller ones. The latter then leads to an overestimation of the effective particle core dimension.

The photoluminescence properties of the CdSe QDs were also investigated. In Figure 2, when excited at 568 nm, the CdSe QDs exhibit a sharp emission peak at 599 nm with a full width at

(44) Brus, L. *J. Phys. Chem.* **1986**, *90*, 2555–2560.

(45) Lide, D. R. *Handbook of Chemistry and Physics*, 76th ed.; CRC: Boca Raton, FL, 1995.

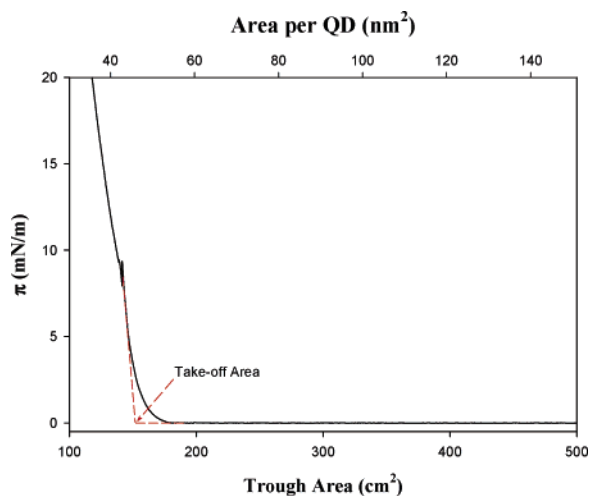


Figure 3. Langmuir isotherm of a CdSe-TOPO monolayer at the air–water interface. Particle concentration $2.7 \mu\text{M}$ in CHCl_3 . Amount spread $220 \mu\text{L}$. Compression speed $10 \text{ cm}^2/\text{min}$. Dashed lines show the extrapolations to define the takeoff area.

half-maximum (fwhm) of only 38 nm, consistent with the narrow distribution of the particle core dimensions as evidenced in TEM measurements. Furthermore, the small difference between the emission peak energy and the absorption edge suggests that the particles behave as direct-band gap materials with minimum surface defects.

Electrochemistry of Langmuir Monolayers. The electronic conductivity of the above CdSe QDs was then examined by voltammetric techniques. First, a CdSe-TOPO monolayer was prepared at the air–water interface by the Langmuir method and an IDA electrode was vertically aligned (Scheme 1) such that we were able to study the QD electron transfer properties in situ at varied interparticle separation. Figure 3 depicts a Langmuir isotherm where the overall feature is quite similar to those observed previously with other metal and semiconductor nanoparticles,^{31–33} with a takeoff area of about 152 cm^2 ($45.9 \text{ nm}^2/\text{QD}$), corresponding to an edge-to-edge interparticle distance of ca. 2.65 nm (assuming a close-packed hexagonal QD array). This is somewhat greater than twice the TOPO ligand chainlength (1.1 nm), as estimated by Hyperchem calculations, which suggests that there exist some structural defects (voids) within the Langmuir monolayer of CdSe-TOPO QDs, since the takeoff area signifies the occurrence of physical contact between the surface ligands of neighboring particles. At a surface area greater than 180 cm^2 , the surface pressure is essentially zero, corresponding to the so-called two-dimensional gas state, whereas with a decreasing surface area, the QD surface ligands between neighboring particles become intercalated, leading to the increase of surface pressure. By controlling the surface pressure, one can readily manipulate the interparticle edge-to-edge distance and hence the interparticle interactions, an important parameter in interparticle charge transfer.

We choose a potential window (-1.0 to $+1.0 \text{ V}$) that is somewhat smaller than the particle band gap (Figure 2). Consequently, in the dark, the voltammetric currents are overall very small ($\sim \text{nA}$), as shown in Figure 4, most likely arising from the few particle surface defects,³² as suggested in the above photoluminescence study (Figure 2). We do see however that, with increasing surface pressure (interparticle separation ranging from >2.65 to 1.76 nm), the voltammetric current increases accordingly, indicating more efficient electron transfer with decreasing interparticle separation, consistent with earlier studies.^{31–34} In addition, the voltammetric profiles exhibited a

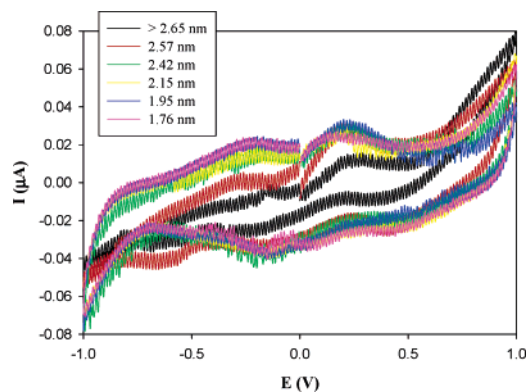


Figure 4. Cyclic voltammograms of the Langmuir monolayer of CdSe-TOPO QDs at varied surface pressures in the dark. The edge-to-edge interparticle separations are shown as figure legends. Potential scan rate 20 mV/s .

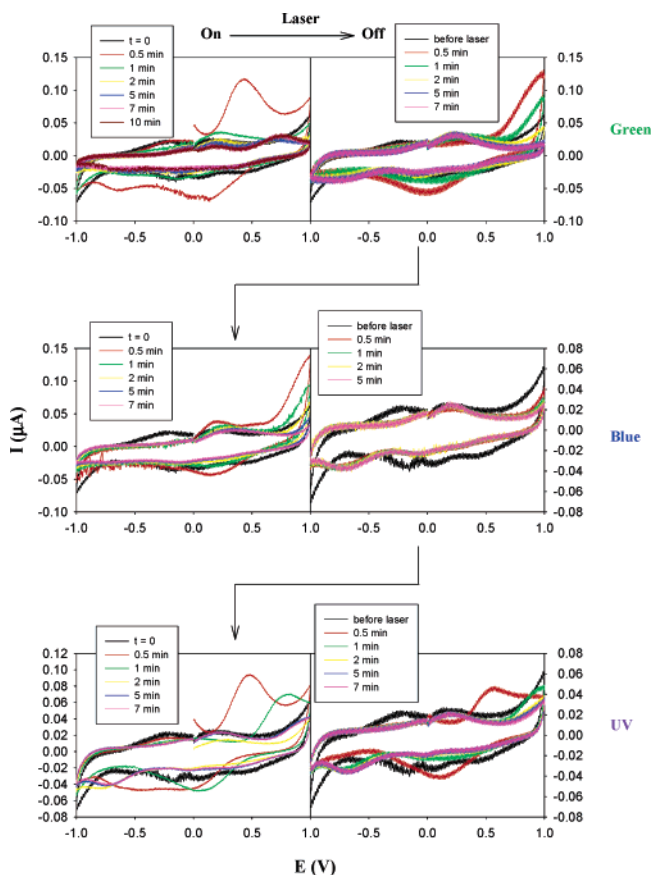


Figure 5. Effects of photoirradiation on the electronic conductivity of the CdSe-TOPO monolayer at an edge-to-edge interparticle separation of about 1.76 nm (same monolayer as in Figure 4). Potential scan rate 20 mV/s . In the left panels, figure legends show the length of time the QD monolayer was exposed to a laser; whereas in the right panels, times shown reflect the period after the laser was turned off. The lasers used are specified in the figures; and arrows indicate the experimental sequence.

point symmetry against the zero potential bias, as one would anticipate from the symmetrical experimental setup and the resulting even distribution of potential across the ensemble.

More interestingly, upon photoexcitation with a low-power laser ($20\sim 25 \text{ mW}$), the voltammetric response exhibits an interesting dynamic transition. Figure 5 top-left panel shows some representative I – V curves with the particle monolayer (edge-to-edge distance 1.76 nm) excited by a green laser (532 nm). Initially a drastic enhancement of the voltammetric current

with a pair of peaks at +0.15 and +0.41 V (red curve, $t = 0.5$ min) can be observed. Since the measurements were carried out with a two-electrode mode and the resistivity of the QD layers was quite high (vide infra), it is most probable that the substantial difference of peak potentials ($\Delta E_p = 0.26$ V) arose largely from the IR drop between the two electrodes. Nonetheless, the symmetrical peak shape suggests that the voltammetric responses might arise from species confined onto the IDA electrode surface and/or adsorbed onto the QD ensemble. In subsequent potential scans, the peak currents decrease quickly (<1 min) with the eventual responses resembling that acquired in the dark (black curve, $t = 0$). It should be noted that the measurements were carried out under ambient conditions; thus, it is very likely that oxygen would adsorb onto the particle surface leading to the formation of surface defects which are known to trap the photogenerated electrons efficiently and hence a lowering of the particle band edge.^{20–23} Consequently, the QD effective band gap increases leading to a decrease of the photoconductivity, as observed experimentally. In addition, the excessive holes may then lead to the oxidative decomposition of CdSe at positive potentials, $\text{CdSe} + 2h^+ \rightarrow \text{Cd}^{2+} + \text{Se}$, where generation and release of ionic species would lead to the formation of a “double-layer” structure at the working electrode. Consequently, the loss of symmetry of the two IDA electrodes leads to the deviation of the voltammetric current profiles from a point-symmetrical behavior that was depicted in Figure 2. Additional effects could arise from the generation of insulating Se which may also lead to the eventual diminishment of the voltammetric current.

Similar observations have been reported previously with other QD molecules where the voltammetric responses were complicated by various experimental parameters including energy of photoexcitation, solvent media, pH, etc.^{20–23,28–30,46} For instance, Park and Barber²⁸ used a Pourbaix diagram to predict the thermodynamic stability of a variety of semiconductor electrode materials. They observed that cadmium chalcogenides (CdE; E = S, Se, or Te) might be unstable by anodic dissolution with varied reaction pathways and generation of different products. A similar mechanism was also suggested to account for the photocorrosion of CdSe films in solar energy conversion studies.⁴⁶ Thus, the observations depicted in Figure 5 suggest that the voltammetric currents measured here most likely arise from a combined contribution of oxygen adsorption (as electron acceptors/scavengers) and the subsequent faradaic decomposition of the CdSe nanocrystals.

By integrating the area of the anodic peak (red curve), one can estimate the total charge passing through the QD film, $1.08 \mu\text{C}$, in CdSe anodic dissolution. If we assume that all this charge arises from the electron-scavenging process of QD-adsorbed oxygen (each accepting four electrons, leading to the excess of equal number of holes), the total number of reactive QD-adsorbed oxygen will be 1.68×10^{12} . With an edge-to-edge interparticle distance of 1.76 nm, there are about 3.45×10^7 QDs trapped between the IDA fingers (this is most probably an overestimation because of voids within the QD monolayer as speculated above in Figure 3). Since the experimental setup is essentially a two-electrode electrochemical cell, cathodic reactions occur at one IDA finger and anodic reactions at the other. Thus, if we assume half of the QDs participate in the cathodic and the other half in anodic reactions, this means that there are about 9.74×10^4 oxygen onto each QD molecule that undergo electrooxidation giving rise to the voltammetric peak. Physically, this is highly unlikely. In other words, the charge associated with the faradaic reactions of the CdSe core is most probably the additional

contributing source (vide ante). However, it remains a challenge to quantitatively assess these two contributions.

Upon cessation of irradiation (top-right panel, Figure 5), the voltammetric currents initially increase slightly (red curve), probably due to some charge separation/collection during the recombination between trapped electrons and holes. However, the currents decrease quickly back to that prior to photoexcitation within a few minutes (black curve), indicating a recovery of CdSe by the reverse reaction with the Cd^{2+} ions still residing at the air–water interface because of the coordination with the freed TOPO ligands. The fact that the eventual voltammetric response is almost identical to that prior to photoexcitation strongly suggests that the oxygen adsorption and related anodic dissolution are highly reversible.

This reversibility is further observed in subsequent experiments with other laser excitations using the same monolayer films (experimental sequence indicated by arrows in Figure 5). Here similar responses were also observed when the same monolayer film was exposed to lasers at higher energies (blue, 473 nm; and UV, 355 nm), as shown in the middle and lower panels of Figure 5. However, the details are somewhat different from those with green laser excitation. For instance, under blue laser excitation (middle-left panel), the initial enhancement of voltammetric currents is significantly smaller (peak area $0.22 \mu\text{C}$) with a pair of anodic and cathodic peaks separated only by $\Delta E_p \approx 40$ mV. However, with UV laser (lower-left panel), the voltammetric peak (peak area $1.0 \mu\text{C}$) in the first potential scan cycle is comparable to that under green irradiation (top-left panel) but with an even larger ΔE_p (≈ 0.5 V). In addition, it is interesting to note that under UV irradiation, in the second potential sweep ($t = 1$ min, green curve), the anodic peak is found to shift anodically. This is consistent with the above argument^{20–23} that oxygen trapping and surface oxidation of the particle cores induce a downward shift in the particle band edge and effectively shrink the particle core diameter. In both cases, the voltammetric currents decrease rapidly and eventually become almost identical to that acquired even before green laser excitation. In addition, when the photoexcitation is turned off, the same dynamic transitions of the I–V responses are observed, namely, a small initial increase followed by a rapid decay back to the original profile, again, indicating the reversibility of the oxygen trapping and particle neutralization. In contrast, with red laser excitation (638 nm) where the photon energy is lower than the absorption threshold, no effect on the voltammetric currents was observed. The exact nature of the discrepancy observed with excitation by different lasers (photon energies) may be, at least in part, ascribed to the effects of photon energies on the dynamics of two competitive mechanisms: charge separation and intraband relaxation. For instance, Bawendi et al.^{47–49} reported that the photocurrent spectral response of a CdSe QD solid film followed the corresponding linear absorption spectrum, independent of applied field and temperature, in particular near the band edge, whereas at higher excitation energies, deviation started to occur which was ascribed to the increase in nonradiative recombination rate of excitons. They argued that charge separation must be a slow process in comparison with the intraband relaxation to the lowest excited state. The results presented herein (Figure 5) imply that the trapping of photoelectrons by adsorbed oxygen is also very sensitive to the specific photon energies.

(47) Leatherdale, C. A.; Kagan, C. R.; Morgan, N. Y.; Empedocles, S. A.; Kastner, M. A.; Bawendi, M. G. *Phys. Rev. B* **2000**, *62*, 2669–2680.

(48) Morgan, N. Y.; Leatherdale, C. A.; Drndic, M.; Jarosz, M. V.; Kastner, M. A.; Bawendi, M. *Phys. Rev. B* **2002**, *66*, 1–9.

(49) Jarosz, M. V.; Porter, V. J.; Fisher, B. R.; Kastner, M. A.; Bawendi, M. G. *Phys. Rev. B* **2004**, *70*, 1–12.

(46) Suleymanov, A. S. *Int. J. Hydrogen Energy* **1991**, *16*, 741–743.

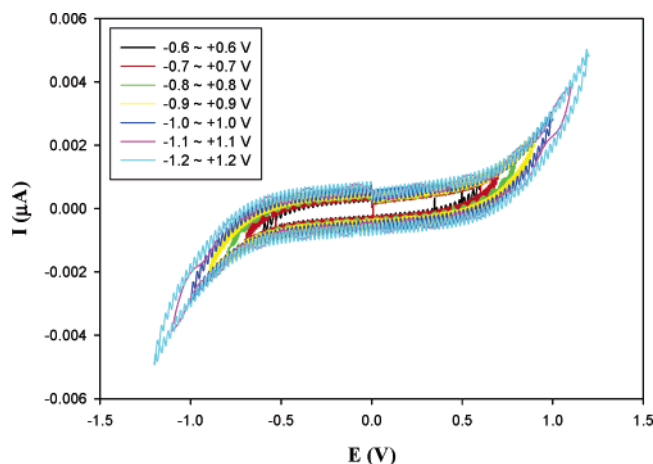


Figure 6. Cyclic voltammograms in the dark and in vacuo of a monolayer of CdSe-TOPO QDs deposited onto an IDA electrode surface by the Langmuir–Blodgett technique. Potential scan rate 20 mV/s.

Overall, although photoexcitation may lead to anodic dissolution of the QD molecules, the almost complete recovery of the voltammetric profiles indicates that the effects due to oxygen adsorption and electron trapping are highly reversible. Such behaviors are in great contrast to our earlier observations with PbS QD monolayers.³² In these earlier studies,³² the PbS QDs were found to undergo both anodic dissolution and cathodic decomposition. Furthermore, the cathodic decomposition was found to be substantially more sensitive to photoexcitation than the anodic process. Consequently, the IDA electrodes were shorted because of deposition of metallic lead onto the electrode surface and the overall I – V profiles were highly irreversible. This seems to imply that in order to achieve a reversible system, one will have to (i) limit the cathodic activities of the QD molecules and (ii) minimize the exposure of the QD ensembles to oxygen.

In comparison, the CdSe QD monolayer was also deposited onto an IDA electrode surface by the Langmuir–Blodgett technique, and the conductivity properties were evaluated in a vacuum such that the oxygen effects would be minimized. Figure 6 shows the corresponding dark currents at varied potential windows where mostly a featureless response was observed except that, when the potential window was expanded beyond -1.0 to $+1.0$ V, a Coulomb blockade started to emerge. Such a behavior has also been observed earlier with other semiconductor QD materials³² where the nonlinear I – V characteristics were ascribed to the weak electronic coupling between neighboring particles, and hence, the particles behaved as isolated entities in charge transfer (the central flat region is a reflection of the effective band gap of the particle ensemble). It should be noted that the overall voltammetric profiles deviated significantly from those in air (Figure 5). In particular, upon photoirradiation with the same lasers used above, the same nonlinear I – V responses were observed with slight increase in currents (not shown), probably because of the low absorbance of the monolayer films. Nonetheless, this behavior is also in sharp contrast to those when the particles were exposed to the ambient atmosphere (Figure 5), again signifying the effects of oxygen in particle chemical stability (and decomposition reactions) as observed above. In addition, our preliminary studies also indicated that increasing temperature led to much more significant enhancement of the CdSe QD monolayers, suggesting a much greater role by thermal activation than by electric field-induced charge separation (i.e., ionization of excitons).^{50–54} More detailed studies are currently underway.

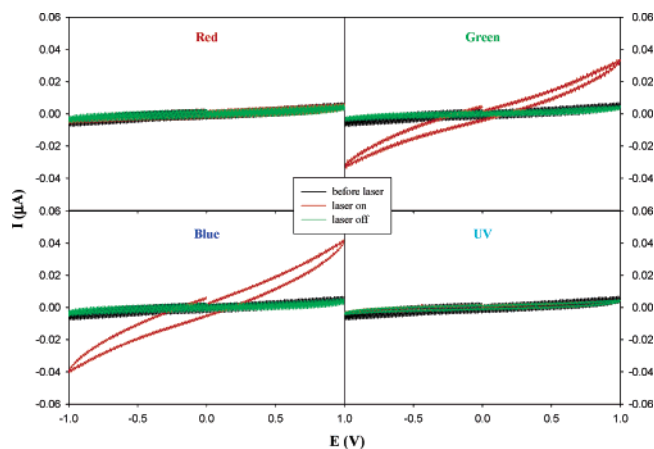


Figure 7. Cyclic voltammograms of a CdSe-TOPO dropcast thick film on an IDA electrode surface in acetonitrile. Potential scan rate 20 mV/s. The voltammograms were acquired before, during and after irradiation by a laser. Four different lasers were used and specified in each panel. It should be noted that a same CdSe QD film was used in these measurements, and the experimental sequence was red \rightarrow green \rightarrow blue \rightarrow UV.

Voltammetry of Dropcast Thick Films. The effect of oxygen was further studied by using QD dropcast thick films immersed into an inert organic media, and a drastic difference of the photoconductivity properties was observed. Here a particle solution was dropcast onto an IDA electrode forming a multilayer of QDs after solvent evaporation (on average, ca. 30 layers; details in the Experimental Section). Figure 7 shows the I – V profile with the QD film immersed into acetonitrile in the absence and presence of photoexcitation at varied energies. Initially in the dark, only a minimum current was observed (on the order of nA, black curves), and under irradiation of a red laser (638 nm), virtually no change was found in the I – V profile (red curve, upper left panel). However, when a green laser (532 nm, upper right panel) was used, the current increased significantly (red curve), and turning off the laser led to an almost complete recovery of the I – V profile (green curve). There are two major differences in terms of the voltammetric features compared to those measured with a QD monolayer at the air–water interface (Figure 5) or the LB monolayer in vacuo (Figure 6). First, the I – V profiles are almost linear with a small charge trapping in the particle film, indicating efficient charge injection from the electrode to the particle films and interparticle charge transfer. Linear I – V responses were also observed with a CdSe QD film in vacuo by Guyot-Sionnest and co-workers⁵³ which were accounted for by the variable range hopping mechanism. Second, the I – V responses are highly stable with rather reproducible conductivity profiles under continuous photoirradiation, in contrast to the dynamic transitions observed above with QD Langmuir monolayers (Figure 5). These observations strongly suggest that the currents measured here may be due to the photoinduced separation of electrons and holes (ionization of excitons) and their collection at the anode and cathode respectively, the fundamental mechanism of a photovoltaic device.^{16–18,55,56} In other words, the CdSe particles are structurally intact under photo- and electrochemical manipulations due to the acetonitrile medium that limits access

(51) Nanda, K. K.; Sahu, S. N. *Appl. Phys. Lett.* **2001**, *79*, 2743–2745.

(52) Yu, D.; Wang, C. J.; Guyot-Sionnest, P. *Science* **2003**, *300*, 1277–1280.

(53) Yu, D.; Wang, C. J.; Wehrenberg, B. L.; Guyot-Sionnest, P. *Phys. Rev. Lett.* **2004**, *92*, 1–4.

(54) Wehrenberg, B. L.; Guyot-Sionnest, P. *J. Am. Chem. Soc.* **2003**, *125*, 7806–7807.

(55) Rajeshwar, K.; de Tacconi, N. R.; Chenthamarakshan, C. R. *Chem. Mater.* **2001**, *13*, 2765–2782.

(56) Nozik, A. J.; Micic, O. I. *Opt. Eng.* **2004**, *87*, 327–385.

(50) Ginger, D. S.; Greenham, N. C. *J. Appl. Phys.* **2000**, *87*, 1361–1368.

Table 1. Variation of the Electronic Conductivity (σ , S/cm) of the CdSe Dropcast Films with Photoirradiation

	red	green	blue	UV
dark (initial state) (S/cm)	4.258×10^{-6}			
laser on (S/cm)	4.83×10^{-6}	3.16×10^{-5}	3.91×10^{-5}	3.11×10^{-6}
laser off (S/cm)	3.34×10^{-6}	3.06×10^{-6}	3.00×10^{-6}	3.13×10^{-6}

^a Note that all data are obtained by linear regressions of the I–V curves in Figure 7.

to ambient oxygen (though not oxygen-free). Similar responses were also observed with the blue laser where the photocurrent was found to be somewhat greater than that with the green laser (red curve, lower left panel). Surprisingly, with the UV laser (355 nm), no appreciable effects were found (lower right panel). This somewhat counterintuitive behavior may be also attributed to the relatively slow charge separation process in comparison with the intraband relaxation, in particular at increasing photon energies, as mentioned earlier.^{47–49}

Quantitative evaluation of the conductivity of the CdSe QD ensembles was achieved by linear regressions of the I–V curves in Figure 7. The results were summarized in Table 1. In the dark or under the irradiation of the red (and surprisingly the UV) laser, the conductivity is of the order of 10^{-6} S/cm, very comparable to that for CdSe thin films.^{57,58} However, under photoexcitation with the green or blue laser, the conductivity increases by about an order of magnitude where the conductivity is slightly greater with the blue laser than that with the green one.

It should be noted that in these measurements (Figure 7) the same QD film was examined. The highly reversible voltammetric responses under photoirradiation indicate that the particle films are structurally intact when access to oxygen is limited, very similar to those with a QD monolayer in vacuo (Figure 6). In comparison, I–V curves were also collected with the QD film exposed in air, and the responses showed dynamic and irreversible transitions similar to those observed in Figure 5 upon photoexcitation at varied energies (not shown), again indicating oxygen-induced chemical instability of the particles.

A similar disparity of the voltammetric profiles between Langmuir monolayers and dropcast thick films was also observed with alkanethiolate-protected gold nanoparticles. For gold

nanoparticles capped with an alkanethiolate monolayer of relatively short chainlength (e.g., butyl or pentyl spacers), the Langmuir monolayers exhibited linear I–V responses; whereas with longer alkyl spacers in the particle protecting layer, nonlinear I–V profiles were observed.^{31,33} This was attributed to the dependence of the interparticle electronic coupling on particle dipole interactions. In contrast, for dropcast (μm) thick films of gold particles, generally only ohmic (linear) behaviors of the I–V measurements were found, regardless of particle surface chainlength (butyl to octadecyl spacers).^{36–41} This behavior was attributed to structural defects within the particle films that facilitate facile electron transfer between neighboring particles. This may also explain the different I–V characteristics that we observed here with CdSe QD dropcast films.

Concluding Remarks

In summary, the electronic conductivity of CdSe-TOPO QD arrays can be sensitively gated by photoexcitation. Oxygen appears to play an important role in the determination of the ensemble voltammetric photocurrents. It was found that the chemical stability of the CdSe QDs and the associated photogated charge transfer mechanism were manipulated by the trapping of photogenerated electrons by adsorbed oxygen. The resulting excess of holes left the particles positively charged and susceptible to photocorrosion (anodic decomposition). The oxygen adsorption and QD photoetching processes were found to be very reversible and sensitive to the specific photon energies. Although it has been known for many years that the electrochemistry at a semiconductor electrode can be sensitively regulated by photoirradiation,⁵⁹ the emergence of new functional nanoparticles and nanostructures offers unprecedented control of their electronic conductivity by taking advantage of their unique quantum confinement effects.^{1–4,60}

We are currently extending the studies to include QDs with varied quantum efficiency or more complicated chemical structures (e.g., core–shell QDs). The related results will be reported in due course.

Acknowledgment. We thank the anonymous reviewers for their helpful critiques and comments. This work was supported in part by an NSF CAREER Award (CHE-0456130), NSF NIRT-0210807, ACS–PRF (39729-AC5M) and UCSC. S.C. is a Cottrell Scholar of Research Corporation.

LA0518851

(59) White, H. S.; Ricco, A. J.; Wrighton, M. S. *J. Phys. Chem.* **1983**, *87*, 5140–5150.

(60) Zhang, J. Z.; Wang, Z. L.; Liu, J.; Chen, S.; Liu, G.-y. *Self-assembled nanostructures*; Kluwer Academic/Plenum Publishers: New York, 2003.

(57) Kale, S. S.; Lokhande, C. D. *Mater. Chem. Phys.* **2000**, *62*, 103–108.

(58) Kale, R. B.; Sartale, S. D.; Chougule, B. K.; Lokhande, C. D. *Semiconductor Sci. Technol.* **2004**, *19*, 980–986.